J Mater Sci: Mater Med (2008) 19:1419–1424
DOI 10.1007/s10856-006-0053-6

Generation of hydroxyapatite patterns by electrophoretic deposition

Seiji Yamaguchi · Takeshi Yabutsuka · Mitsuhiro Hibino · Takeshi Yao

Received: 10 August 2006 / Accepted: 20 November 2006 / Published online: 4 October 2007

Abstract Hydroxyapatite (HAp) patterns with distinct boundaries were generated by electrophoretic deposition (EPD) utilizing an insulating mask that partially blocks the electric field. For the EPD process, we selected two types of mask: a polytetrafluoroethylene (PTFE) board with holes and a resist pattern. A porous PTFE film, which differed from the mask PTFE, was employed as a substrate and attached to the mask. EPD was performed with a suspension of wollastonite particles in acetone, which were deposited on the substrate in the form of the patterned mask. The deposited wollastonite particles induced HAp patterns during a soak in simulated body fluid (SBF). As a result, minute HAp patterns, such as dots, lines, and corners were fabricated on the porous PTFE substrate with a minimum line width of about 100 μm.

Introduction

Micron- and nano-scale patterns, made of bioactive and biocompatible materials, have recently drawn great interest in the medical field. The proliferation and differentiation of cells on such patterns have been studied at the single cell level based on the hypothesis that a fine pattern may copy the complicated environments found in a living body. It has become clear that surface characteristics, including surface chemistry and surface topography, have a significant influence on adhesion, morphology, and maturation of cultured cells [1–5]. Moreover, the generation of fine patterns can be combined with various functional materials at a micron scale and can contribute to the development of biochips, which are useful for biotechnology including genomics, proteomics, computational biology, and pharmaceuticals [6–12]. Advances in these areas provide additional methods to help the comprehenstion of the complex biochemical processes occurring inside cells [13, 14].

Hydroxyapatite (HAp) has a high affinity for bone, cells, and viruses [15–17]. The formation of HAp patterns may be an excellent method to develop smart biomaterials using the bioaffinity of HAp. For example, patterns of living cells can be cultured on a patterned HAp substrate. This method may be applicable to the development of a cellular biosensing system. Further, biosensing devices can be developed using the adsorbability of HAp to biomolecules such as proteins.

Electrophoretic deposition (EPD) is widely used for the deposition of ceramic particles and has many advantages, including a simple process, inexpensive apparatus, and ability to use substrates with wide areas and complicated shapes [18, 19]. Although EPD has been applied only to electric conductive substrates, such as metals, both conductive and nonconductive materials are often used as biomaterials. The use of EPD with insulating materials will promote its utilization in the biomedical field. Recently, we have found that when a porous insulating material is arranged between EPD electrodes, ceramic particles can be migrated by passing an electric field through the pores [20].

S. Yamaguchi (✉) · T. Yabutsuka · M. Hibino · T. Yao
Graduate School of Energy Science, Kyoto University, Yoshida, Sakyo-ku, Kyoto 606-8501, Japan
e-mail: S.Y@esi.mbox.media.kyoto-u.ac.jp

T. Yabutsuka
e-mail: Takeshi@t27a2136.mbox.media.kyoto-u.ac.jp

M. Hibino
e-mail: hibino@energy.kyoto-u.ac.jp

T. Yao
e-mail: yao@energy.kyoto-u.ac.jp

This method enables us to deposit various ceramic particles on porous insulating materials.

For biomedical applications, EPD has been used to generate dense and porous HAp coating films on metallic substrates such as titanium [21–24]. Wang et al. have patterned HAp onto a conductive substrate including titanium by EPD [25]. As a cathode, they employed a metallic substrate on which another type of metal was patterned. When voltage was applied, the electric current density patterned across the cathode and HAp particles were preferentially deposited on the areas with higher electric current density. The authors concluded that the difference in electric field across the two metals on the cathode enhanced HAp patterning through an electrohydrodynamic process [25–27]. Although the potential and flexibility of EPD in patterning charged particles onto a substrate was demonstrated by this study, a clear HAp pattern with distinct boundaries, which is preferable for biochip and scaffolding applications, has still not been fabricated by EPD. The purpose of the study reported herein is the formation of minute and complicated HAp patterns with distinct boundaries on a porous insulating substrate by EPD. First, we verified a method for generating clear HAp patterns using drilled polytetrafluoroethylene (PTFE) board as a mask, in which holes allow for the EPD electric field. Next, we determined that the attachment of a porous substrate to an electrode that is partially covered with insulating material blocked the deposition of ceramic particles onto areas where the electric field is blocked. Consequently, a negative pattern of particles is formed on the substrate. Therefore, we attempted the facile preparation of an HAp pattern with complicated and fine-scale structure by utilizing a minute resist pattern developed by photolithography, a standard technique in the semiconductor industry.

Experimental

Hydroxyapatite patterns were generated in two stages, an EPD process and a biomimetic process (Fig. 1). First, bioactive wollastonite particles were deposited by EPD in the form of a mask partially blocking the electric field. Next, bonelike HAp was selectively induced on the wollastonite by a biomimetic method. The details of each process are described below.

Wollastonite synthesis

Silicon dioxide was preheated at 1000 °C for 2 h and mixed with calcium carbonate in an equimolar ratio. Wollastonite was synthesized by calcination of this mixture at 1500 °C for 5 h, and was subsequently pulverized with a laboratory planetary-type ball mill (Model p7. Fritsch). X-ray diffraction determined that the final product was

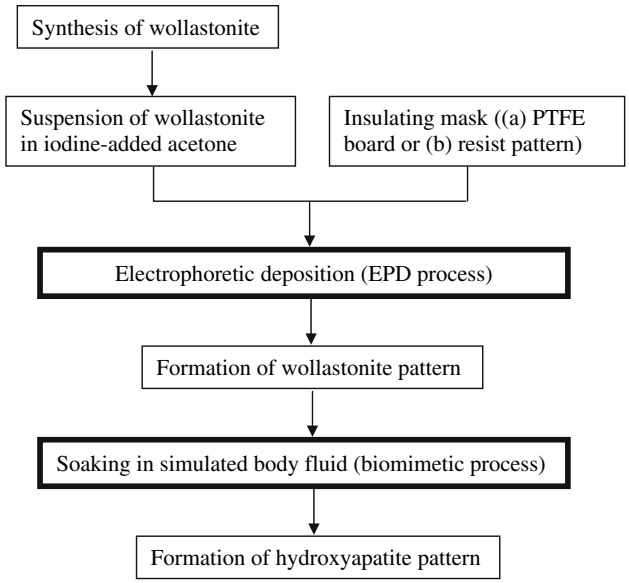

Fig. 1 Diagram of HAp patterning by EPD and subsequent biomimetic process. (**a**) and (**b**) are masks used in the EPD process for the verification test and fabrication of fine structure, respectively

α-wollastonite, a known bioactive material [28]. The median size of the particles was about 3 μm as measured by particle size analyzer (LA-700, HORIBA).

Electrophoretic deposition (EPD)

Verification test

We drilled minute holes thorough a 2 mm thick PTFE board to generate a circular pattern of holes that was 100 μm in diameter. This PTFE board was used as a mask, and the holes allowed penetration of the EPD electric field. A porous PTFE film, 25 mm in diameter, 0.07 mm in thickness, 0.1 μm average pore size, and 68% porosity, was employed as a substrate and attached to the mask. Though both the mask and substrate are made of PTFE, their features are significantly different: the former is a dense board with drilled holes and the latter is a porous film. We prepared iodine-containing acetone at a concentration of 0.10 g dm^{-3} and suspended the wollastonite particles in this solution at 5.0 g dm^{-3}. Gold plates of $30 \times 30 \times 0.5$ mm were used as both an anode and a cathode. These electrodes were separated by 20 mm, and the masked substrate was arranged between them. EPD was performed at 1000 V constant voltage for 1 min.

Fabrication of fine structure

Commercial photoresist (AZ1500, Clariant (Japan)) was spin-coated onto a stainless steel plate and baked at 100 °C for 1 min. The thickness of the resist layer was measured at

about 2.4 μm by scanning electron microscopy (SEM; ESEM-2700, Nicon). The resist was exposed through a photomask to UV light of 436 nm for 2.7 s and developed in a NaOH solution (10 g dm^{-3}). The photomask included dot, line, and corner patterns. We confirmed that the resist was patterned after the UV irradiation and rendered insoluble to acetone by thermal treatment at 250 °C for 20 min [29, 30]. This thermal treatment did not change the thickness of the resist layer. The stainless steel plate with the resist pattern was used as a cathode. A porous PTFE film, similar to that used in the verification test, was employed as a substrate and attached to the cathode. Wollastonite particles were suspended in acetone solution containing a small amount of iodine. The concentrations of wollastonite particles and iodine were 5.0 and 0.10 g dm^{-3}, respectively. A gold plate of 30 × 30 × 0.5 mm was used as an anode and was set 20 mm from the cathode. EPD was performed at a constant 200 V for 4 min.

Treatment with simulated body fluid (SBF)

Simulated body fluid (SBF) [31] was prepared by dissolving reagent-grade NaCl, $NaHCO_3$, KCl, $K_2HPO_4{\cdot}3H_2O$, $MgCl_2{\cdot}6H_2O$, $CaCl_2$, and Na_2SO_4 (Hayashi-Junyaku Industry) in ultrapure water followed by buffering to pH 7.40 with tris(hydroxymethyl)aminomethane ($(CH_2OH)_3CNH_2$) and 1 M aqueous HCl solution (Hayashi-Junyaku Industry) at 36.5 °C; the concentrations in the resulting solution were nearly equal to those of human blood plasma (Na^+142.0, K^+5.0, Ca^{2+}2.5, Cl^-147.8, HCO_3^-4.2, HPO_4^{2-}1.0, and SO_4^{2-}0.5 mmol dm^{-3}). Following EPD, the porous PTFE substrate was soaked in the SBF for 24 h, removed from the fluid, and air dried.

Analysis of surfaces and cross sections of specimen

The surfaces and cross sections of the porous PTFE substrate were studied by thin film X-ray diffraction (TF-XRD; Rint 2500, Rigaku), SEM, and energy dispersive X-ray analysis (EDX; DX-4, Edax International).

Results and discussion

First, we discuss the results of verification test to verify the method for generating distinct HAp patterns. Figure 2 shows an SEM micrograph and the results of EDX mapping of the porous PTFE substrate following EPD. Particles were deposited on the substrate in the form of the dot pattern of the mask (Fig. 2a). EDX mapping (Fig. 2b and c), detected the Ca and Si characterizing wollastonite ($CaSiO_3$) in the same areas, indicating that the dot pattern consists of wollastonite particles. It has been reported that charged particles are swept into regions of higher current density through an electrohydrodynamic mechanism [26, 27]. In this test, the wollastonite particles were preferentially deposited on areas where the electric field passed through the holes in the PTFE-board mask. Some scattering signals were also observed between patterns (Fig. 2b and c), indicating that wollastonite particles were deposited between patterns. The cross section of the wollastonite pattern is shown in Fig. 3a. The thickness of the pattern was approximately 6 μm, corresponding to the deposition of five or six layers of composite particles of approximately 1 μm diameter in size. The pattern was maintained after the PTFE board was removed from the acetone solution, indicating that the deposited particles agglutinated properly due to hydrodynamic effects resulting from electroosmosis during EPD [32, 33]. Next, the substrate was soaked in SBF for 24 h. A TF-XRD profile following the SBF soak is shown in Fig. 4b. The TF-XRD profile of an untreated porous PTFE substrate is also given as a reference (Fig. 4a). Following the SBF soak, a peak around 26° appeared on the substrate. It is known that bonelike HAp is formed on bioactive materials in SBF [34]; therefore, we conclude that the wollastonite particles induced HAp formation. Figure 5a shows an SEM micrograph of an HAp dot, verifying that it has a distinct boundary. The thickness of the HAp layer was determined by SEM to be about 6 μm (data not shown). This thickness can be controlled by adjusting the length of soaking in SBF [35]. Figure 6 shows an SEM micrograph and the results of EDX mapping of the PTFE substrate after the SBF soak. In Fig. 6a, a dot pattern of about 250 μm diameter was observed. Figure 6b and c show that Ca and P that characterize HAp were detected in the same area. However, the Si attributed to wollastonite was not detected (data not shown). These results indicate that HAp was induced by wollastonite and replaced it during the SBF soak. The mechanism of HAp formation in this study may be similar to that observed on $CaO–SiO_2$-based glass and glass ceramics reported by Kokubo, et al. [36].

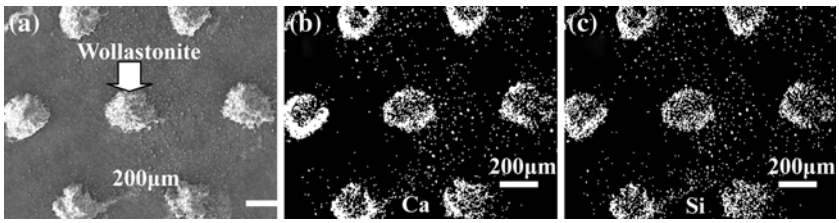

Fig. 2 (**a**) SEM micrograph and (**b**), (**c**) results of EDX analysis of the anode side surface of the porous PTFE substrate after EPD in the verification test

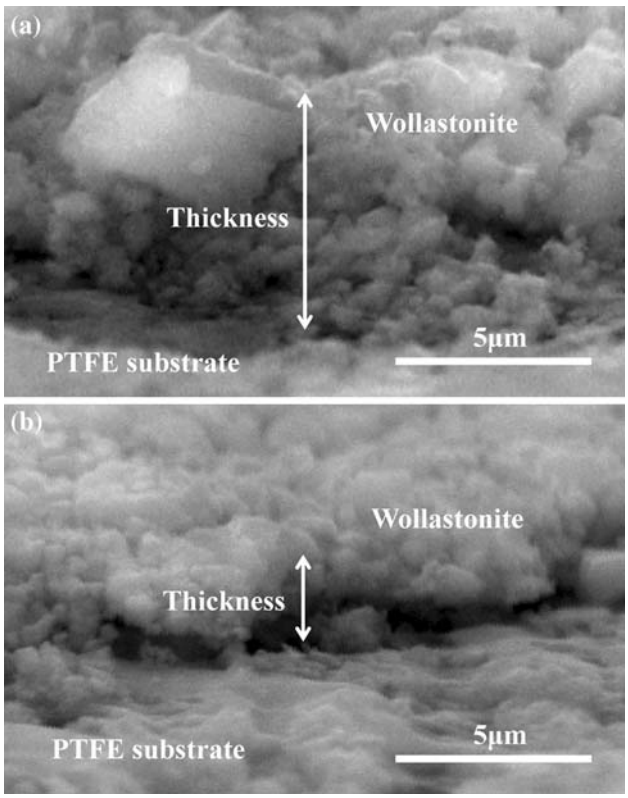

Fig. 3 SEM micrographs of the cross section of the wollastonite pattern in (**a**) the verification test and (**b**) fabrication of fine structure

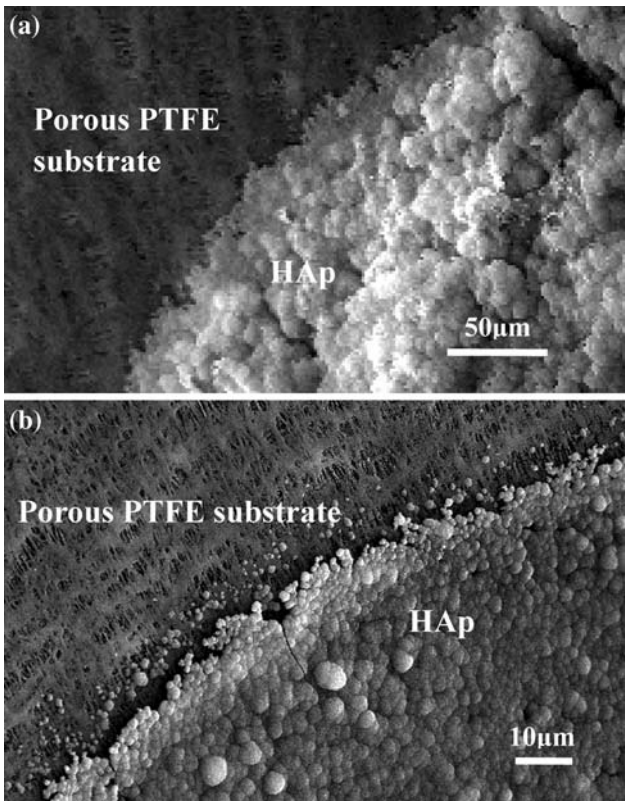

Fig. 5 SEM micrograph of the boundary of HAp dots after SBF soak (**a**) in the verification test and (**b**) in fabrication of fine structure

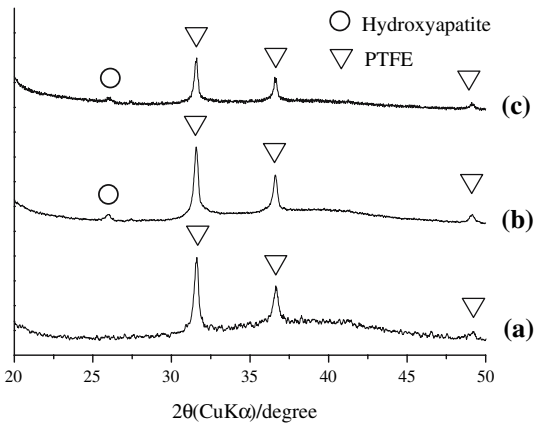

Fig. 4 TF-XRD profiles of the anode side surface of the porous PTFE substrate after a 24 h SBF soak (**b**) in the verification test and (**c**) in fabrication of fine structure. The TF-XRD profile of a porous PTFE substrate is given as a reference in (**a**)

The calcium ion dissolved from the wollastonite increases the ion product of HAp in the surrounding fluid, and the hydrated silica on the surface of the wollastonite provides favorable sites for rapid HAp nucleation. Once HAp nuclei form on the wollastonite, they spontaneously grow by consuming calcium and phosphate ions from the surrounding fluid. The size of the HAp pattern was almost the same as that of the wollastonite pattern. It should be noted that EDX mapping did not detect scattering signals following the SBF soak because the disaggregated wollastonite particles deposited between the patterns during EPD dissolved in the SBF prior to HAp induction. Therefore, an HAp dot pattern with distinct boundaries was generated by EPD and subsequent soaking in SBF.

Next, we show the results of the fabrication of fine structure, in which we attempted the facile preparation of complicated and fine HAp patterns by utilizing a resist

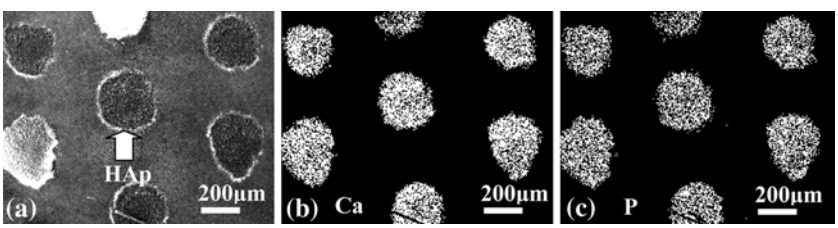

Fig. 6 SEM micrograph and results of EDX analysis of the anode side surface of the porous PTFE substrate after a 24 h SBF soak in the verification test

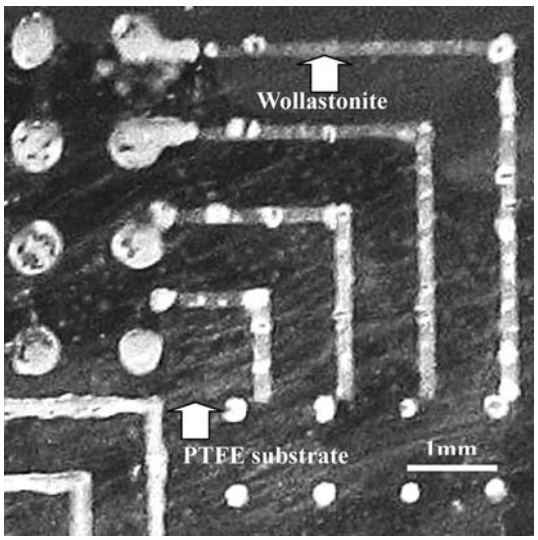

Fig. 7 Photograph of the anode side surface of the porous PTFE substrate after EPD in fabrication of fine structure

pattern. Figure 7 shows a photograph of the porous PTFE substrate following EPD. Dot and corner patterns that followed the resist pattern were observed. As shown in Fig. 3b, the thickness of the pattern was 3 μm, thinner than that observed in the verification test. This difference is due to adjustments in the EPD conditions: applied voltage and process time. Moreover, the size of the deposited particles was smaller than that in the verification test, indicating that the lower voltage resulted in preferential deposition of fine particles. A similar phenomenon has been reported in other studies [21, 37]. EDX mapping of the patterns are shown in Fig. 8. Ca and Si were detected in the same areas, as shown in Fig. 8b–c and e–f. These results indicate that wollastonite particles were not deposited onto areas where the electric field was blocked by the resist pattern. In other words, wollastonite particles were deposited onto areas with higher current density, as was expected. The substrate was next soaked in SBF. TF-XRD detected an HAp peak on the substrate (Fig. 4c), indicating that HAp was formed during the SBF soak. Figure 9 shows SEM micrographs and the results of EDX mapping of the porous PTFE substrate after the SBF soak. Dot and line patterns can be observed in Fig. 9a and d. EDX mapping (Fig. 9b–c and e–f) detected Ca and P in the same areas, indicating that HAp was selectively induced on the wollastonite deposits by the mechanism discussed above. SEM observations

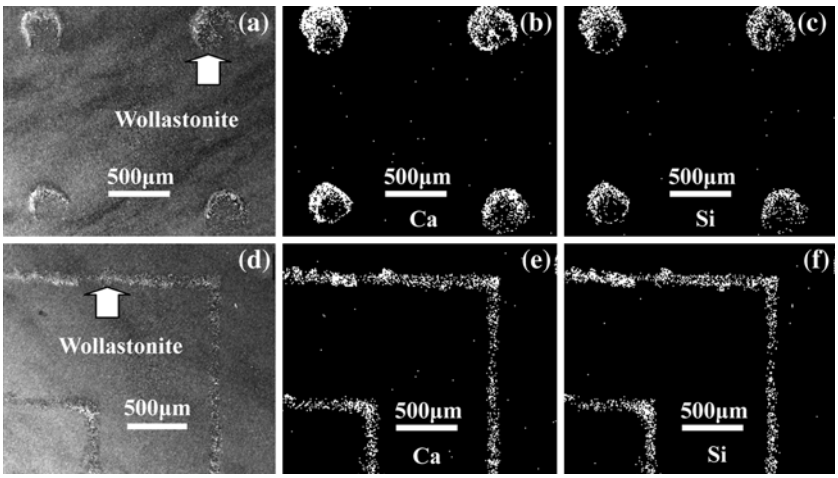

Fig. 8 SEM micrographs and results of EDX analysis of the anode side surface of the porous PTFE substrate after EPD in fabrication of fine structure

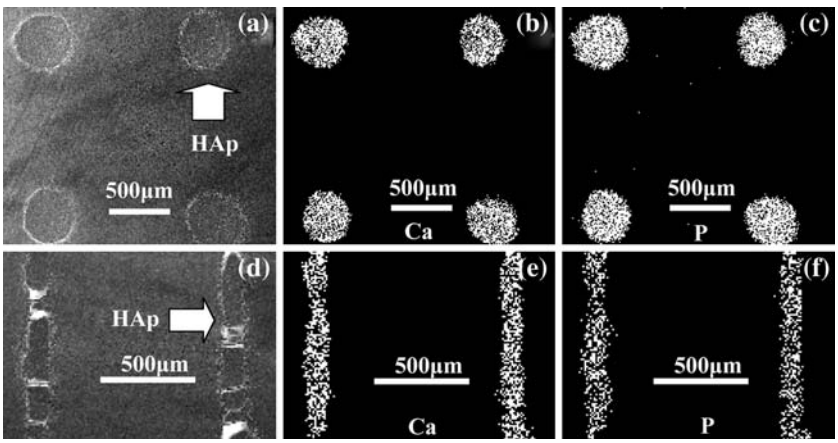

Fig. 9 SEM micrographs and results of EDX analysis of the anode side surface of the porous PTFE substrate after a 24 h SBF soak in fabrication of fine structure

(figure not shown) showed that the HAp layer was about 6 μm thickness, which was comparable with that in the verification test. In addition, the formed patterns had distinct boundaries (Fig. 5b). As shown in Fig. 9a, a line width of about 100 μm was obtained—this resolution is as fine as the original resist pattern. According to other reports, patterns with size ranging from tens to hundreds of μm and from several to tens of μm are used for biochip and topographic studies, respectively [1, 2, 38]. Thus the HAp patterns generated in this study fit for biochip. Moreover, finer HAp patterns for topographic studies will be generated utilizing finer resist patterns as masks and optimizing EPD conditions.

Conclusions

We successfully used EPD and biomimetic methods to generate HAp patterns with distinct boundaries on porous PTFE substrate using a PTFE-board mask. Furthermore, we demonstrated the fabrication of minute HAp dot, line, and corner patterns by utilizing a resist-pattern mask in the EPD process. Using this method, we expect to be able to generate more complex and fine HAp patterns that will be useful in the production of multifunctional materials with bioaffinity.

References

1. H. LIAO, A. S. ANDERSSON et al., *Biomaterials* **24** (2003) 649
2. F. PFEIFFER, B. HERZOG et al., *Microelectron. Eng*. **67**, (2003) 913
3. L. F. COOPER, T. MASUDA et al., *Int. J. Oral. Maxillofac. Implants*. **13**, (1998) 163
4. J. E. DAVIES, *Anat. Rec*. **245** (1996) 426
5. T. MASUDA, P. K. YLIHEIKKILA et al., *Int. J. Oral. Maxillofac. Implants*. **13**, (1998) 17
6. J. COOPER, Y. WANG et al., *Electrophoresis*. **25** (2004) 3913
7. P. J. OBEID, T. K. CHRISTOPOULOS et al., *Anal. Chem*. **75** (2003) 288
8. G. H. W. SANDERS and A. MANZ, *TRAC Trends Anal. Chem*. **19** (2000) 364
9. R. GOMEZ, R. BASHIR et al., *Biomed. Microdevices*. **3** (2001) 201
10. I. R. LAUKS, *Acc. Chem. Res*. **31** (1998) 317
11. J. KŘUGER, K. SINGH et al., *J. Micromech. Microeng*. **12** (2002) 486
12. J. VOLDMAN, M. L. GRAY et al., *Annu. Rev. Biomed. Eng*. **1** (1999) 401
13. A. KOLCHINSKY and A. D. MIRZABEKOV, *Hum. Mutat*. **19** (2002) 343
14. W. KUSNEZOW, Y. V. SYAGAILO et al., *Expert Rev. Mol. Diagn*. **6** (2006) 111
15. M. KUSUNOKI, M. KAWASHITA et al., *Jpn. J. Appl. Phys*. **44**(10) (2005) 326
16. P. ZHU, Y. MASUDA and K. KOUMOTO, *Biomaterials*. **25**(17) (2004) 3915
17. G. YIN, Z. LIU, J. ZHAN, F. DING and N. YUAN, *Chem. Eng. J*. **87**(2) (2002) 181
18. W. F. PICKARD, *J. Electorochem. Soc*. **115** (1968) 105
19. P. SARKAR and P. S. NICHOLSON, *J. Ame. Ceram. Soc*. **79**(8) (1996) 1987
20. T. YAO, N. OZAWA, Y. IDETA and K. SHIMIZU, *Bioceramics*. **15** (2003) 67
21. I. ZHITOMIRSKY and L. GAL-OR, *J Mater. Sci-Mater. M*. **8** (1997) 213
22. J. HAMAGAMI, Y. ATO and K. KANAMURA, *J Ceram. Soc. Jpn*. **114** (2006) 51
23. J. MA, C. WANG and K. W. PENG, *Biomaterials*. **24**(20) (2003) 3505
24. M. WEI, A. J. RUYS, B. K. MILTHORPE, C. C. SORRELL and J. H. EVANS, *J. Sol-Gel. Sic. Techn*. **21** (2001) 39
25. R. WANG and Y. X. HU, *J. Biomed. Mater. Res. A*. **67**(A) (2003) 230
26. M. TRAU, D. A. SAVILLE et al., *Science*. **272** (1996) 706
27. M TRAU, D. A. SAVILLE et al., *Langmuir*. **13** (1997) 6381
28. P. N. De AZA, Z. B. LUKLINSKA, M. R. ANSEAU, F. GUITIAN and S. De AZA, *J. Dent*. **27** (1999) 107
29. S. K. KURINEC and E. SLUZKY, *J. Soc. Inform. Display*. **4**(4) (1996) 371
30. J. H. YUM and Y. E. SUNG, *J. Electrochem. Soc*. **51**(2) (2004) H27
31. T. KOKUBO, H. KUSHITANI, S. SAKKA, T. KITSUGI and T. YAMAMURO, *J. Biomed. Mater. Res*. **24** (1990) 721
32. Y. SOLOMENTSEV, M. BÖHMER and J. L. ANDERSON, *Langmuir*. **13** (1997) 6058
33. M. BÖHMER, *Langmuir* **12** (1996) 5747
34. K. HATA, T. KOKUBO et al., *J. Ame. Ceram. Soc*. **78**(4) (1995) 1049
35. P. LI, C. OHTSUKI, T. KOKUBO, K NAKANISI and N. SOGA, *J. Am. Ceram. Soc*. **75**(8) (1992) 2094
36. C. OHTSUKI, T. KOKUBO and T. YAMAMURO, *J. Non-Cryst. Sosids*. **143** (1992) 84
37. X. W. MENG, T. Y. KWON, Y. Z. YANG, J. L. ONG and K. H. KIM, *J. Biomed. Mater. Res. B*. **78B**(2) (2006) 373
38. D. SPICER, J. N. MCMULLIN and H. ROURKE, *J. Micromech. Microeng*. **16** (2006) 1674